Materials Research. 2014; 17(4): 1056-1064
DOI: http://dx.doi.org/10.1590/1516-1439.278114

3D Finite Element Modeling of Grains Refinement for Magnesium Alloys by Extrusion-shear and Experimental Verification

Hu Hongjun[a,b]*, Zhai Zhiye[a], Li YunYang[a], Wang Hao[a], Fan JunZhi[a], OU zhongwen[b]

[a]College of Material Science and Engineering, Chongqing University of Technology, Chongqing, 400050, China
[b]The PLA Chongqing Logistics Engineering College, 401311, China

Received: March 3, 2014; Revised: May 25, 2014

To explore the deformation mechanisms of a new composite extrusion including extrusion and successive shear subsequently which is shorten "ES", Three dimensional finite element modeling of grain refinements for magnesium alloys by ES process has been researched. The ES die have been designed and manufactured and installed to the horizontal extruder. Finite element software DEFORM™-3D to investigate the plastic deformation behaviors of magnesium alloy during extrusion-shear has been employed. The extrusion loads and temperatures distribution of billets and maximum extrusion forces have been obtained from simulation results. From the simulation results it is clear that evolutions of extrusion loads curve and effective stresses and temperatures can be divided into three stages. ES process has been applied to fabricate AZ31 magnesium alloy rod at preheat temperature of 420°C with extrusion speed of 20 mm/s. The results proved that the ES process is a formality method for magnesium suitable for large scale industrial application. The microstructures of AZ31 magnesium alloy along the longitudinal section of rods have been sampled and examined and observed. Fine grained microstructures can be observed throughout longitudinal section of extruded rod. The researches results show that ES process would cause severe plastic deformation and improve the dynamic recrystallization of AZ31 magnesium alloy. The simulation results and calculated Zener-Hollomon parameters showed that the grains of magnesium would be refined gradually during ES process.

Keywords: *AZ31 magnesium alloy, finite element modeling, grain refinement, dynamic recrystallization, extrusion load, effective stress, temperature evolution*

1. Introduction

Magnesium (Mg) alloys have been used in transportation, communications, electronics and aerospace etc., and have become the focus concerned by all the countries in the world[1,2]. Its specific strength and rigidity are superior to iron and aluminum. The greatest limitation for the usage of wrought magnesium is its poor formability at room temperature. Because of its hexagonal closed packed (HCP) crystal structure and only two independent basal slip systems can be activated[3,4]. So more than 90% of the Mg alloys currently are applied in cast state. In the future development of Mg alloys will rely on large scale production applications of wrought Mg alloy products. But deformation capacity and strength for the traditional extruded rods of Mg alloy is rather poor[5,6].

In recent years, bulk nanostructure materials processed by severe plastic deformation (SPD) such as equal channel angular pressing (ECAP) have attracted the growing interest of specialists in materials science[7-9]. The ECAP process is only used in the laboratory scale processing and preparation for nanocrystalline material, but the technology is not widely used in the industrial field. The main obstacle to spread the use of ECAP in industrial manufacturing is low productivity, ECAP usually involves a large number of steps and is not easily applied from the laboratory to an industry for it is not a continuous process, and the length of extruded rod is the same big as the initial billet. Although it has been invented in the early 1980s, the process did not develop as much as one would desire and is still confined to the laboratory scale experiments. Matsubara K et al.[10] used a new processing procedure to extrude a cast Mg-9% Al alloy involving the sequential application of extrusion and equal channel angular pressing. Experiments showed that the Mg-9% Al alloy has an initial grain size of ~50μm after casting but this was reduced to ~12μm after extrusion and it was further reduced to ~0.7μm when the extruded alloy was subjected to ECAP for 2 passes at 473 K. Although the cast alloy exhibits extremely limited ductility and the extruded alloy was only moderately ductile. It was demonstrated that processing by EX-ECAP produces excellent superplastic ductility including the occurrence of both low temperature superplasticity and high strain rate superplasticity. But EX-ECAP usually includes more than 2 steps, and the material endures intricate diversification of forming environments including process temperatures and may be oxidized. Matsuyama et al.[11] introduced the feasibility of SPD techniques which combines conventional extrusion and equal channel angular pressing into a single process. The

*e-mail: *e-mail: 48516686@qq.com

extruded material exhibits an excellent balance of strength and tensile ductility. But severe plasticity deformation technologies are difficult to be promoted to industrialize, and the processes are very complicated, and costs are high. The ES may improve the industrialization preparation and processing of Mg alloy rods.

To illustrate the potential industrial application of the ES extrusion, we designed and manufactured the ES dies installed on the horizontal extruder, and the experiments of ES process have been done. The microstructures of AZ31 Mg alloy sampled from as-received in ES formed rods have been observed and analyzed. Deformed microstructure evolutions of the ES process for AZ31 Mg alloy have been studied in order to analyze the deformation mechanisms of ES extrusion. The aim of the present study is to reveal the microstructure evolution and clarify the grain refinements mechanism in AZ31 during ES process. The present study employs finite element software DEFORM™-3D to simulate the effective stresses, extrusion forces and temperatures evolution during ES process. The microstructures evolutions and dynamic recrystallizations during period of extrusion and shear of Mg alloy have been researched.

2. Simulation Conditions of ES Process for AZ31 Mg Alloy

A commercial wrought alloy AZ31B (as-cast, Mg-3%Al-1%Zn, w.t. %) was used in the simulation and extrusion experiments. The extrusion tooling consisting of die, container and ram was made of the H13 hot-work tool steel. The physical properties of AZ31B are given in Table 1. The curves of specific heat and thermal conductivity dependent on temperature are shown in Figure 1a and Figure 1b respectively. The present study adopts the following assumptions[8]: (1) both the container and the die are rigid bodies, (2) the extrusion billet is a rigid-plastic material, and (3) the friction factors between the extrusion billet and the ram, container, and die are constant.

2.1. *Flow stress curves for AZ31 Mg alloys*

As-cast AZ31B rods with a diameter of 50 mm were used as the initial material in this study. Cylindrical specimen with a diameter of 10mm and a height of 12 mm were machined from the rods with their longitudinal axis in parallel with the pre-extrusion direction. Axial compression testing for hot workability analysis was carried out using a Gleeble1500D machine[9]. Graphite foils were placed between the specimen and platens for lubrication. At a constant strain rate ranging from 0.01 to 10 s^{-1} and at an initial temperature between 250 and 500°C. The specimen was resistance-heated through a thermocouple sending feedback signals to control the AC-current. The flow stress curves measured in these tests were corrected and a set of flow stress-strain curves are shown in Figure 2 as examples with strain rates 0.1s^{-1} and the different pre-set temperatures 250°C and 300°C and 350°C and 400°C. The data were input into the material property module of the DEFORM™-3D software.

Table 1. Physical properties of the AZ31 workpiece.

Property	Mg alloy AZ31
Heat transfer coefficient between tooling and billet (N/ °C s mm^2)	11
Heat transfer coefficient between tooling/ billet and air (N/ °C s mm^2)	0.02
Poisson's Ratio	0.35
coefficient of linear expansion ($°C^{-1}$)	26.8E-6
Density (kg/m^3)	1780
Poisson's ratio	0.35
Young's modulus (Mpa)	45000
Emissivity	0.12

2.2. *Contact and friction boundary conditions*

To represent the friction behavior the generalized coulomb's law was used. The friction between the workpiece and die was considered as shear-type[10]. It was well known that the shear is proportional to the contact pressure and the relationship is shown in Equation 1.

$$\tau = \mu \frac{\sigma}{\sqrt{3}} \quad (1)$$

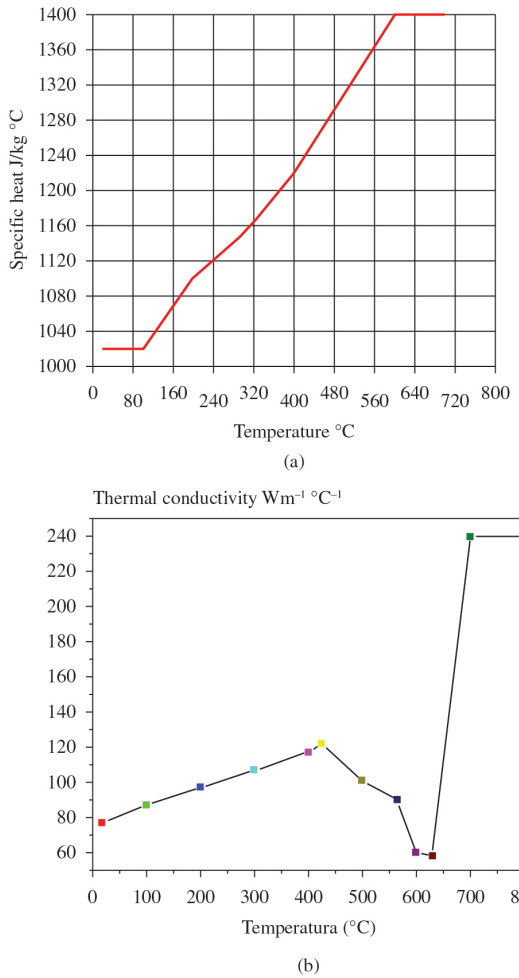

Figure 1. Curves of material properties with different temperatures for AZ31 Mg alloy, (a) specific heat and (b) thermal conductivity.

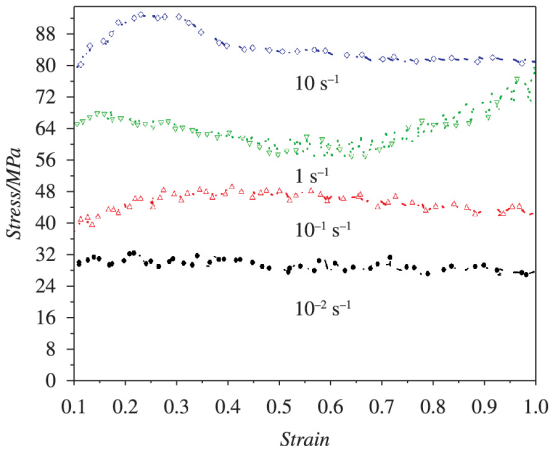

Figure 2. True stress/true strain curves obtained from the compression tests with pre-set temperature 400°C and the different strain rates $0.01s^{-1}$-$10s^{-1}$.

Table 2. Simulation and experimental parameters.

Billet length /mm	100
Billet diameter /mm	59
Container insider diameter /mm	60
Container outside diameter (mm)	84
Die bearing length (mm)	5
Extrusion ratio	14.7
Initial tooling temperature (°C)	400
Ram speed (mm/s)	20
Friction factor of the container–billet interface	0.7
Friction factor between the billet and die.	0.7
Total number of elements	20000
Mesh density type	Relative
Relative interference depth	0.7
Initial billet temperature (°C)	420

where τ is the frictional shear stress and σ is the effective flow stress of the workpiece. μ ($0 \leq \mu \leq 1$)the friction factor .

2.3. *The coefficient of heat transfer between AZ31 Mg alloy and die*

Table 2 presents the simulation and experimental parameters. The ambient temperature was set as 20°C, and temperature of the ES die is 400°C.The initial billet temperature was chosen to be at a relatively high level 420°C. Heat transfer coefficient between tooling and billet was 11 N/°Cs mm^2, and the value of heat transfer coefficients between tooling/billet and air are 0.02 N/°Cs mm^2[11,12]. Emissivity coefficients of the AZ31 and H-13 tool steel were 0.12 and 0.7 respectively. ES extrusion experiments were carried out to verify the results obtained from computer simulation in laboratory. In order to validate the results of finite element analysis, ES dies were designed and manufactured to perform the actual extrusion processes.

3. Experiments

To certify the industrial applications of ES extrusion, the ES die with two shearings has been designed and manufactured. Figure 3 presents the schematic diagram of the experiment. The longitudinal section schematic diagrams of ES extrusion are schematically shown in Figure 4. The die includes direction extrusion with extrusion ratio 32 and two steps ECAP with 120° corner angle. By two steps ES extrusion, a larger amount of shear deformation can be introduced than the direct extrusion with the same extrusion ratio. The deformation zone can be divided into 4 zones, which are the reducing zone, the sizing zone, the first shearing zone, the second shearing zone respectively. The billets and the die in experiments had identical geometrical parameters and material with those in simulations. AZ31 Mg materials and the ram and the lubricated die would be preheated in the furnace for 2 hours before the actual

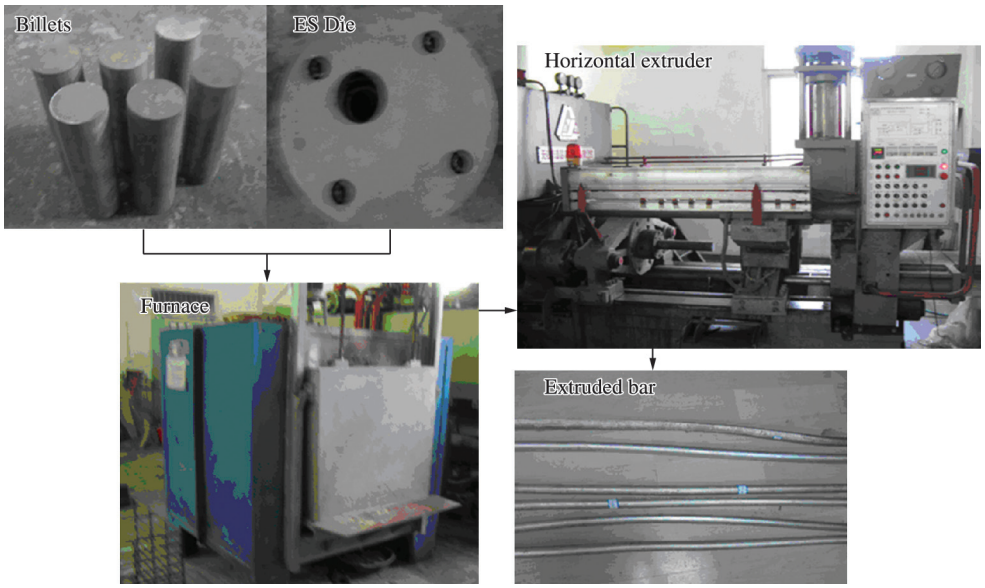

Figure 3. Schematic diagrams of forming steps during ES process.

ES process started. The ES extrusion was then employed to extrude the Mg alloy rods. Before extrusion the billets were machined to a diameter of 80 mm. Real extrusion experiments were carried out by employing a 500 Ton press with a resistance heated container and a heater. The die material, die dimensions, billet dimensions and extrusion conditions were all the same as those used in numerical simulation. The billet was heated in an external furnace up to 420°C and transported into the container at a preset temperature of 420°C to avoid too much heat dissipation and then ES process started immediately. Ram speed was 20 mm/s during experimental verification.

In this study, samples have been taken from the four parts which locations are indicated in Figure 4. All the samples have been taken from the center of rod. We used acetic acid to erosion surface of the samples for microstructure observations by using PME OLYMPUS TOKYO-type optical microscope.

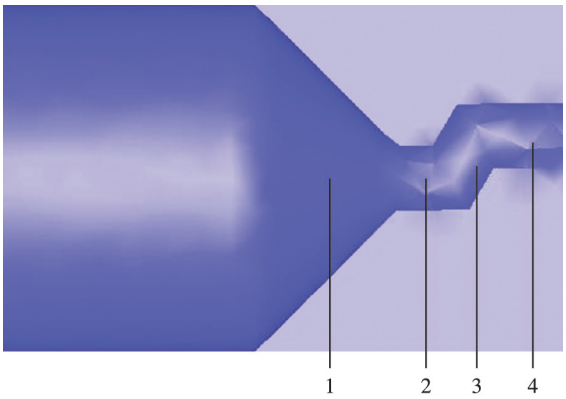

Figure 4. Schematic diagram of ES die with two 120° corner angles and extrusion ratio 32: 1-the reducing zone; 2- the sizing zone; 3-the first shearing zone; 4-the second shearing zone.

4. Results and Discussion

4.1. *The curves of load and time*

The curves of extrusion loads varying with extrusion time during ES process have been described in Figure 5. The values for maximum extrusion forces were obtained from the finite element simulation results. The extrusion load curve can be divided into three stages which include the extrusion upsetting stage and the direction extrusion stage and continuous shears stage. At the initial stage of the extrusions process, the billet was subjected to severe plastic deformation if billet contact with die corners. And the load increases rapidly to 1 MN, this stage is not steady. And subsequently the load decrease somewhat, the billets are continuously extruded through the corners of the die. Further, the deformation load decrease as the entire billet is entered into the deformation zone. During the third phase the load oscillates and the average value is about 1.08 MN. The maximum deformation load is as such as 1.2 MN, and the ES process is in the steady-stage. It is necessary to understand the distributions and magnitudes of effective stresses are analyzed during ES process. However, the extrusion loads also decrease the die life.

4.2. *The distributions of effective stresses during ES process*

Examination of the predicted strains provides quantitative insight into the deformation behaviors of billet during ES process. Figure 6 shows the evolutions of

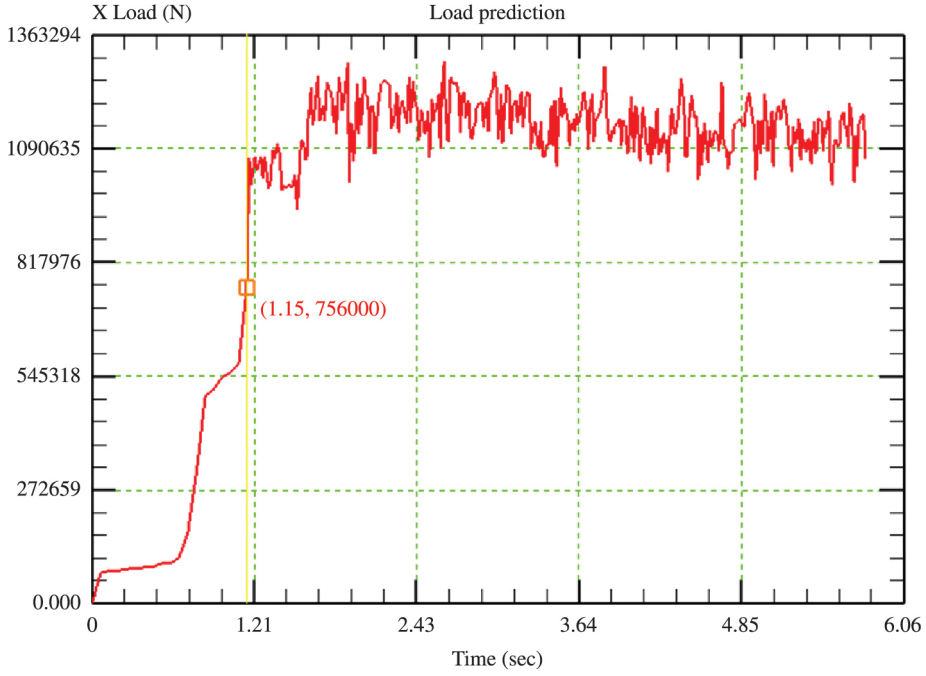

Figure 5. The extrusion loads during ES extrusion.

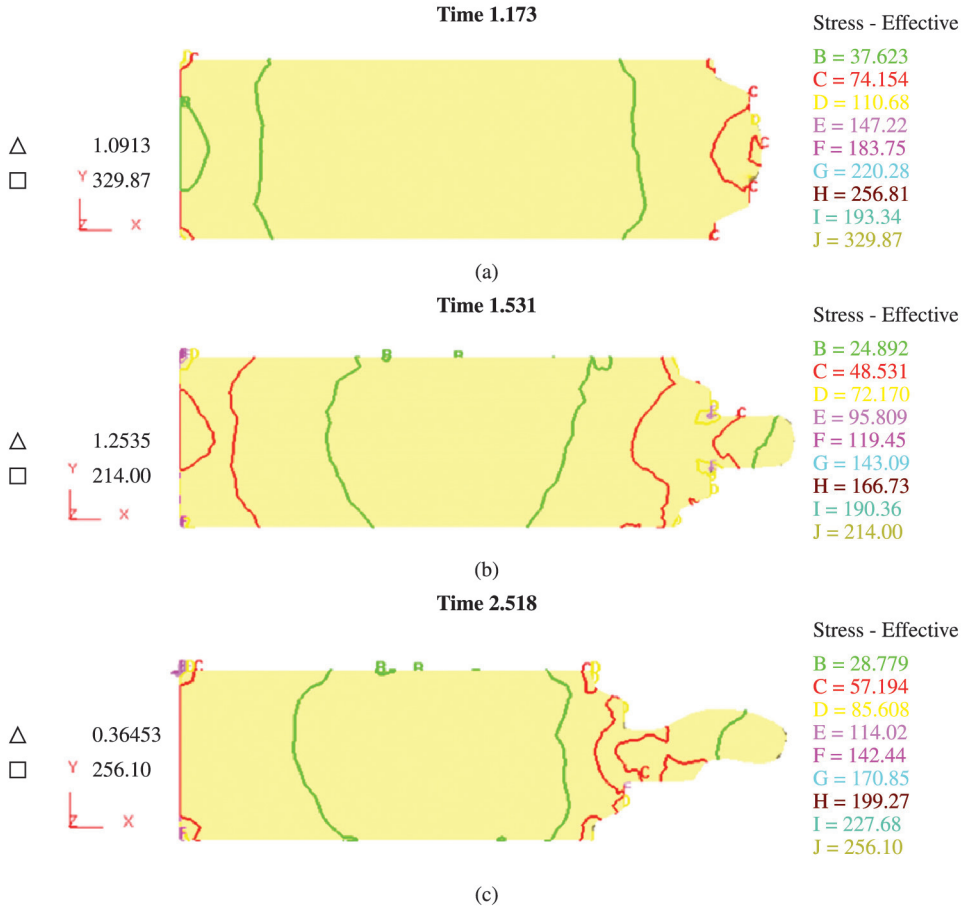

Figure 6. the evolutions of effective stress contours in Mg billet during different ES steps.

effective stress contours in Mg billet during different ES steps, which provide the important information of the stress distribution. Figure 6a, 6b and 6c are the distributions of the equivalent stress for extrusion time 1.173 s, 1.531 s and 2.518 s respectively. The effective stresses of the material are not even seen from the Figure 6, and the maximum effective stress is about 74.154MPa at extrusion time 1.173 s. The deformation of the initial extrusion is inhomogeneous, and the highest stress (48.531MPa) from Figure 6b locate at outer corner at extrusion time 1.531s. Distributions of the stress are lamellar with distinct deformation gradients. The deformation of this position is close to simple shear deformation. But the stresses concentrate upon deformation zone at the extrusion time 2.518 s in Figure 6c. It can be found that the effective stresses in the workpiece decrease with developments of the ES process for the dynamic recrystallization take place during ES process.

4.3. *Temperature evolution during ES process*

The temperature is highest during ES process at the material/die interface due to friction force. The temperature distribution inside the billet during ES process is uneven due to heat generation and friction between the workpiece/ES dies and heat exchange between the ES die and the environment. Figure 7a displays the temperature isotherm during upsetting extrusion stage at a ram speed of 20 mm/s. It is clear that the temperatures of surface in the billet decrease slightly comparing initial extrusion temperature. The main feature of the temperature evolution at this phase of ES process is that the temperature in the rear part away from the die entrance decreases gradually. As the process proceeds, the temperature distributions do not change too much. At this stage, the heat dissipation through tooling is greater than heat generation from ES process, the billet temperature descends gradually. Figure 7b and 7c show the temperature isotherm distributions during steady-state of ES process. The minimum temperature locates at the edge of the billet between the container and the die face for a lot of heat is emission and less heat generated in the deformation zone.

The temperatures of the billet in the deformation zone increase. The temperature rise is result of heat generation from deformation energy and friction heat, and heat exchanges inside the billet, with the ES die and the environment. It seems that heat flow in two reverse directions. One heat flow tends to increase the billet temperature and the other to decrease the billet temperature.

The curves of maximum and minimum temperature in the workpiece throughout the ES process at a ram speed of 20 mm/s are shown in Figure 8. The maximum temperatures in the workpiece rise from 420°C to 435°C during extruding the magnesium alloy into rod.

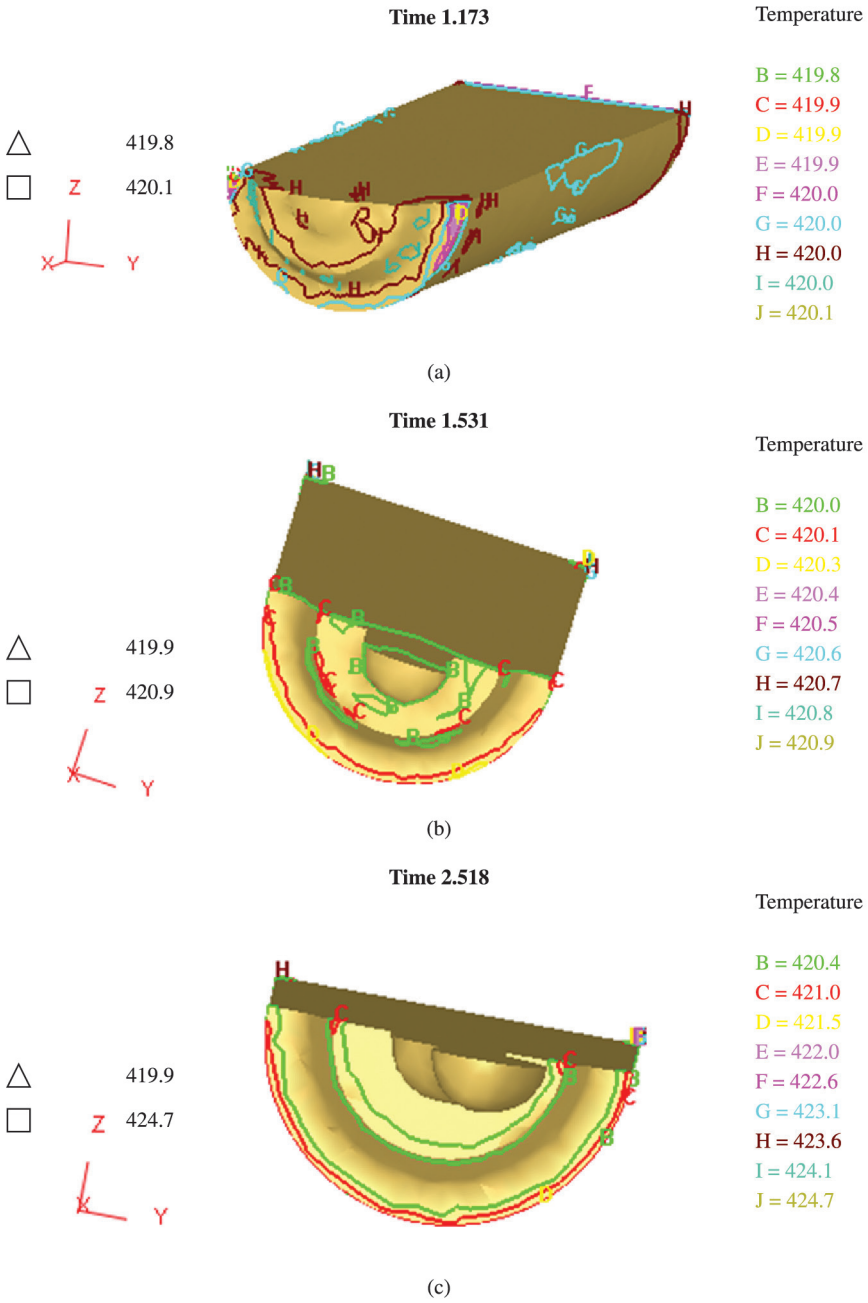

Figure 7. The evolutions of temperature contours in Mg billet during different ES steps.

4.4. *Microstructure evolutions during ES extrusion*

Figure 9 shows microstructures for as-received AZ31 alloy in Figure 9a, and microstructures about four parts in rod formed by ES process shown in Figures 9b, 9c, 9d and 9e respectively. The average grains size of as-received as cast AZ31 alloy is about 250 μm in Figure 9a. The microstructures appear long strips shown in Figure 9b in the extruded reducing zone of ES process. This indicates that the deformation degree is small. The uniform deformation takes place in the grains mainly and improves the formation of rod-like microstructures in Figure 9c, meanwhile part dynamic recrystallization occur between a small number of grains. As the deformation continues, the width of the rod-like microstructures become narrow, a number of twin crystals lamellar-structure appear in the grains shown in Figure 9c and dynamic crystallization has taken place. Rod-like and lamellar microstructures in first shear zone shown in Figure 9d begin to be reduced for the large shear strain caused by shear deformation in this zone and the deformation grains are turned into recrystallization grains.

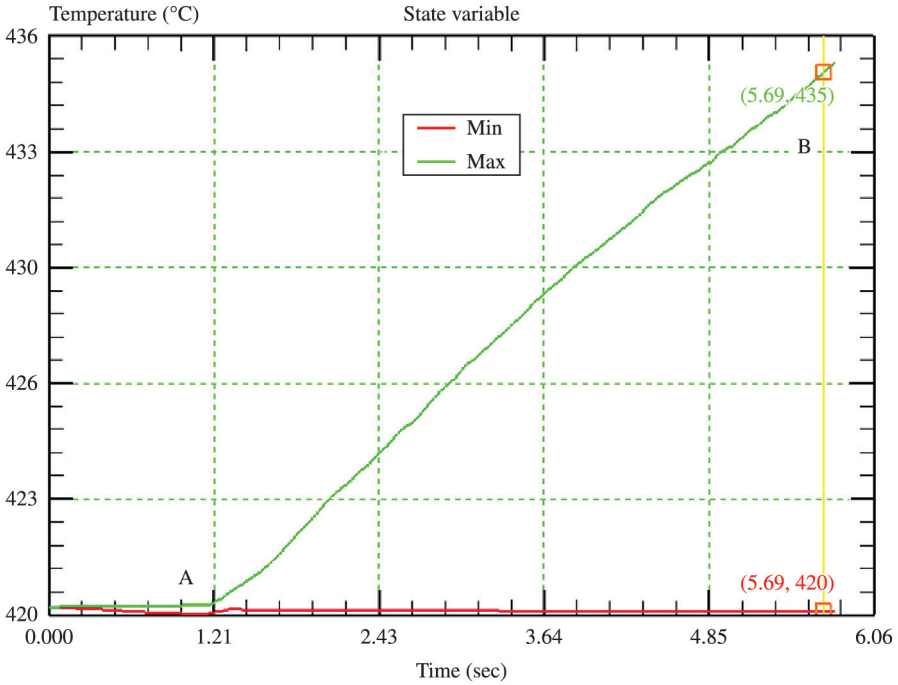

Figure 8. Maximum and minimum temperature in the workpiece throughout the ES process.

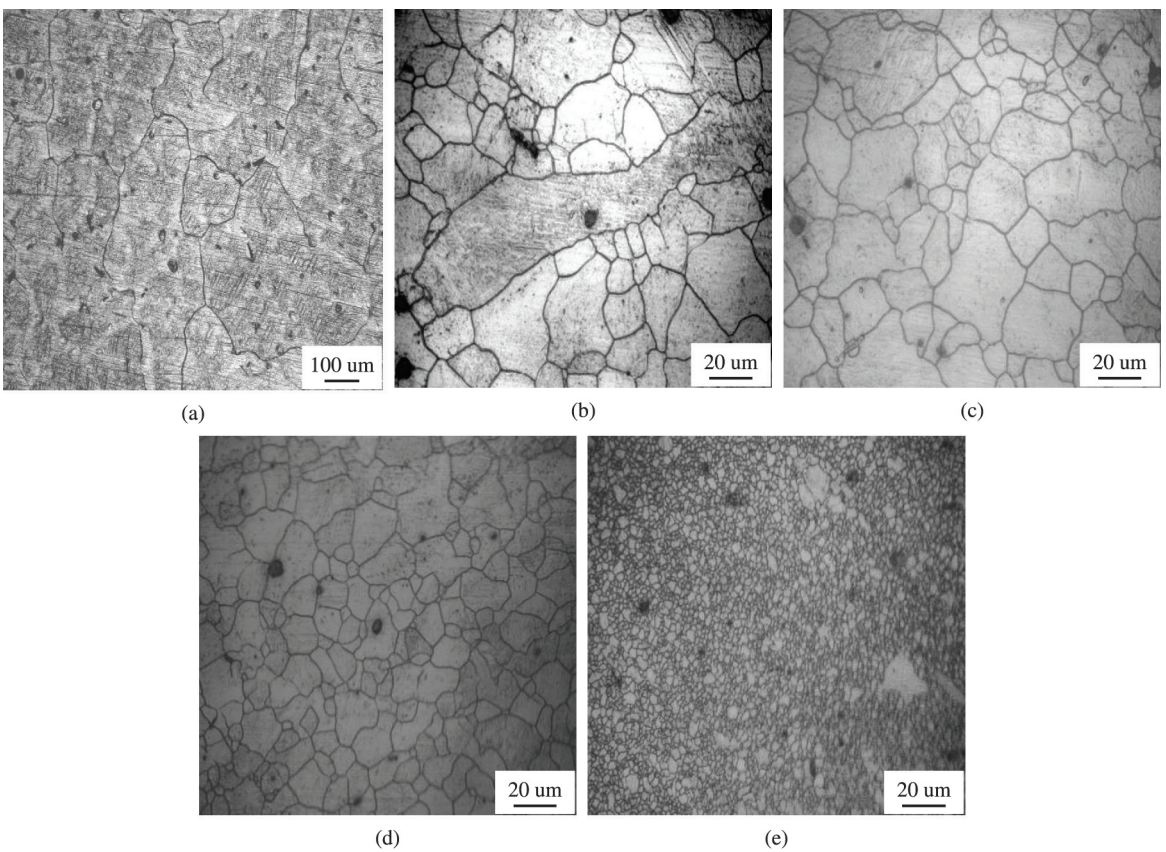

Figure 9. Microstructures for as-received AZ31 alloy (a) and microstructures in different parts of ES die, (b) reducing zone, (c) sizing zone, (d) the first shear step and (e) the second shear step.

In the secondary shear zone, dynamic recrystallization is sufficient for twice shearing later, but there are still a small amount of fine-grain bar in the center of the rod shown in Figure 9e. There were some inherent drawbacks for microstructures of extrusion process due to uneven metal flow during extrusion and the properties from surface to the center were uneven. But the use of ES process, the average grain size can be changed from 250 μm to 5 μm. The microstructures are not only clearly refined but also relatively uniform. This is because the ES process include two successive simple shear processes more than a direct extrusion. So that the deformation degree of central part of rods increases, the part recrystallizations occur. Therefore, the microstructures become smaller and more homogeneous.

4.5. *Dynamic recrystallization during ES extrusion*

The principle of ES process is to introduce compressive and accumulated shear strain into the Mg alloy. The character of ES process is that the sample is subjected to two shear deformations. The accumulative strains of ES extrusion can be expressed as Equations 2 which include two parts: accumulative strain of direct extrusion and two continuous ECAP steps[10,13] .

$$\varepsilon = \ln\lambda + 2*\left[\frac{2\cot(\frac{\phi}{2}+\frac{\psi}{2})+\psi\csc(\frac{\phi}{2}+\frac{\psi}{2})}{\sqrt{3}}\right] \quad (2)$$

where ε is the accumulative strain; λ is the extrusion ratio; Φ is the inner corner angle, Ψ is the outer corner angle. The relationship between the average recrystallization grain size (d) and the Zener-Hollomon parameter (Z) during dynamic recrystallization is given by Equation 3[13].

$$Z = \dot{\varepsilon}\exp(\frac{Q}{RT}) \quad (3)$$

Where έ is strain rate, Q is the activation energy for the deformation, T is the temperature and R is the gas constant.

Dynamic recrystallization (DRX) is one of the interesting mechanisms of microstructure evolution. Grain refinement could be attributed to continuous dynamic recrystallization which involves a progressive increase in grain boundary disorientation and changes of low angle boundaries into high angle boundaries. The Zener-Hollomon parameter (Z) of first direct extrusion is equal to Z_1. v_1 is the extrusion speed. λ is the extrusion ratio, R1 is the billet radius[14]. The parameters were substituted into Equation 3 the Equation 4 is obtained[15,16].

$$Z_1 = \frac{3v_1}{R_1}\ln\lambda\exp(\frac{Q}{RT}) \quad (4)$$

And the Z parameters of first and second shearing are Z_2 and Z_3 respectively[17-19].

$$Z_2 = Z_3 = \left[\frac{2\cot(\frac{\phi}{2}+\frac{\psi}{2})+\psi\csc(\frac{\phi}{2}+\frac{\psi}{2})}{\sqrt{6}}\right]\frac{\sqrt{v_2}}{\psi R_2}\exp(\frac{Q}{RT}) \quad (5)$$

Where inner corner angle (Φ), outer corner angle (ψ). V_1 is the speed of extruded rods. R_2 is radius of extruded rod.

The relationship between the average recrystallization grain size (d) and the Z during dynamic recrystallization is given by -lnd= A + Bln Z. Based on the present ES processing with extrusion temperature 420°C, average accumulative strains, strain rates and Z parameters of the AZ31 samples in different positions are listed in Table 3. It can be found that the accumulative strain increase with the extrusion advancing, so the grains will be refined consequently. It is clear that there are three phase recrystallization during ES process. It can be found that the average sizes of grains for DRX were coarsened with the preheating temperature increasing and Z parameter decreases with the temperature.

5. Conclusions

This study utilized three-dimensional finite element DEFORM software and ES process to investigate the plastic deformation behaviors of Mg billets during ES process with ES combination die. The coupled thermo-stress finite element models including the mathematical models and geometric models and solution conditions have been applied to calculate the effective stresses and temperatures and required extrusion forces during ES process. The results have been shown as following.

The extrusion load curve can be divided into three stages including the extrusion upsetting stage and the direction extrusion stage and continuous shears obtained from simulation results. During the third phase the load oscillate about an average value about 1.08 MN. The maximum deformation load is as such as 1.2 MN, and the ES forming is in the extrusion steady-stage.

The ES die structures have been manufactured and installed to the horizontal extruder. ES forming was applied to fabricate AZ31 Mg alloy rod at preheat temperature of 420°C with speed of 20mm/s. The results proved that the ES extrusion is a formality method for Mg suitable for large-scale industrial application. The microstructures along forming direction were examined. ES extruded AZ31 sample showed a fine-grained microstructure throughout longitudinal section. The ES extrusion would cause severe plastic deformation and improve the dynamic recrystallization during ES extrusion. The microstructures show that ES is an efficient and inexpensive grain refinement method for Mg alloys. Zener-Hollomon parameters during

Table 3. Theory Calculation results for dynamic recrystallization during ES process.

Temperature	ε_1	ε_2	ε_3	$\dot{\bar{\varepsilon}}_1$	$\dot{\bar{\varepsilon}}_2$	$\dot{\bar{\varepsilon}}_3$	Z_1	Z_2	Z_3
420°C	3.47	4.12	4.8	2.45	1.51	1.51	2.52	1.33	1.33

ES process showed that the grains of Mg would be refined gradually.

Acknowledgements

This work was supported by the open fund for Key Laboratory of Manufacture and Test Techniques for Automobile Parts (Chongqing University of Technology) Ministry of Education in 2013, and National Science of China (Grant No. 51101176) and foundation of the post doctorate in Chongqing city and Project Number is Xm201327, and China Postdoctoral Science Foundation funded project, and Natural Science Foundation Project of cstc2014jcyjA0133.

References

1. Hu H, Zhang D and Zhang J. Microstructures in an AZ31 magnesium alloy rod fabricated by a new SPD process based on Physical Simulator. *Transactions of Nonferrous Metals Society of China*. 2010; 20(3):478-483.
2. Gong X, Li H, Kang SB, Cho JH and Li S. Microstructure and mechanical properties of Twin-roll Cast Mg-4.5Al-1.0Zn alloy sheets processed by differential speed rolling. *Materials and Design*. 2010; 31(3):1581-1587. http://dx.doi.org/10.1016/j.matdes.2009.09.021
3. Hu H, Huang WJ and Wu GS. 3D finite element modelling and experimental researches on turning steel AISI1013 by nano-crystalline Al2O3 ceramics cutter. *International Journal of Machining and Machinability of Materials*. 2013; 14(3):295-310. http://dx.doi.org/10.1504/IJMMM.2013.056369
4. Orlov D, Raab G, Torbjorn T, Lamark, Popov M and Estrin Y. Improvement of mechanical properties of magnesium alloy ZK60 by integrated extrusion and equal channel angular pressing. *Acta Materialia*. 2011; 59(1):375-385. http://dx.doi.org/10.1016/j.actamat.2010.09.043
5. Gong X, Kang SB, Li S and Cho JH. Enhanced plasticity of twin-roll cast ZK60 magnesium alloy through differential speed rolling. *Materials & Design*. 2009; 30(9):3345-3350. http://dx.doi.org/10.1016/j.matdes.2009.03.040
6. Hu H, Zhang D, Yang M and Deng M. Grain refinement in AZ31 Magnesium alloy rod fabricated by an ES SPD process. *Transactions of Nonferrous Metals Society of China*. 2011; 21(2):243-249. http://dx.doi.org/10.1016/S1003-6326(11)60705-X
7. Gong X, Cheng B, Price S and Chou K. Powder-bed electron-beam-melting additive manufacturing: powder characterization, process simulation and metrology. In: *Proceedings of the ASME District F Early Career Technical Conference*; 2013; Birmingham, United States. p. 59-66
8. Hu H, Zhang D, Pan F and Yang M. Analysis of the cracks formation on surface of extruded magnesium rod based on numerical modeling and experimental verification. *Acta Metallurgica Sinica: English Letters*. 2009; 22(5):353-364. http://dx.doi.org/10.1016/S1006-7191(08)60109-X
9. Gong X and Chou K. Characterizations of sintered Ti-6Al-4V powders in electron beam additive manufacturing. In: *Proceedings of the ASME 2013 International Manufacturing Science and Engineering Conference*; 2013; Madison, United States.
10. Matsubara K, Miyahara Y, Horita Z and Langdon TG. Developing superplasticity in a magnesium alloy through a combination of extrusion and ECAP. *Acta Materialia*. 2003; 51(11):3073-3084. http://dx.doi.org/10.1016/S1359-6454(03)00118-6
11. Matsubara K, Miyahara Y, Horita Z and Langdon TG. Achieving enhanced ductility in a dilute magnesium alloy through severe plastic deformation. *Metallurgical and Materials Transactions A*. 2004; 35(6):1734-1744. http://dx.doi.org/10.1007/s11661-004-0082-z
12. Hu H. The effects of special extrusion on the grain refinements of magnesium alloy. *International Journal of Microstructure and Materials Properties*. 2013; 8(6):436-446. http://dx.doi.org/10.1504/IJMMP.2013.059479
13. Hu H, Yang M, Gong X and Li G. Optimization of casting processes based on computer numerical simulation. *Ordnance Material Science and Engineering*. 2006; 29(6):51-53.
14. Wu G, Hu H, Gong X, Zhang W, Wang K and Dong T. application and development of casting process parameterized graph library based on AutoCAD software. *Foundry Technology*. 2007; 28(4):535-537.
15. Liu Gang, Zhou J and Duszczyk J. Finite element simulation of magnesium extrusion to manufacture a cross-shaped profile. *Journal of Manufacturing Science and Engineering*. 2007; 129(3):607-614. http://dx.doi.org/10.1115/1.2714590
16. Hu H. The effects of process parameters on evolutions of thermodynamics and microstructures for composite extrusion of magnesium alloy. *Advances in Materials Science and Engineering*. 2013; 2013:1-9. http://dx.doi.org/10.1155/2013/259594
17. Gong X, Anderson T and Chou K. Review on powder-based electron beam additive manufacturing technology. In: *Proceedings of the ASME 2012 International Symposium on Flexible Automation*; 2012; St. Louis, United States. p. 507-515.
18. Qin F, Gong X and Chou K. Size effects in cutting with a diamond-coated tool. In: *Proceedings of the ASME 2011 International Manufacturing Science and Engineering Conference*; 2011; Corvallis, United States. p. 267-273. http://dx.doi.org/10.1115/MSEC2011-50234
19. Yang M, Qin C and Pan F. Effects of heat treatment on microstructure and mechanical properties of Mg-3Sn-1Mn magnesium alloy. *Transactions of Nonferrous Metals Society of China*. 2011; 21(10):2168-2174. http://dx.doi.org/10.1016/S1003-6326(11)60990-4